Geophysical Research Letters

Key Points:

- Nighttime vapor pressure deficit increased >50% in 40 years over the foothills of the Sierra Nevada and Rocky Mountains
- Saturation vapor pressure increases caused by rising temperatures and decreases in actual vapor pressure account for these changes
- The magnitudes of the changes in the observation-based records greatly exceed those projected by climate forecast models

Multi-Decadal Change in Western US Nighttime Vapor Pressure Deficit

Andrew M. Chiodi[1,2] , Brian E. Potter[3], and Narasimhan K. Larkin[3]

[1]Joint Institute for the Study of the Atmosphere and Ocean, University of Washington, Seattle, WA, USA, [2]National Oceanographic and Atmospheric Administration Pacific Marine Environmental Laboratory, Seattle, WA, USA, [3]Pacific Wildland Fire Sciences Laboratory, USDA Forest Service, Seattle, WA, USA

Abstract Amid reports from western US wildland fire managers that, compared to when many started their careers, fires are burning longer throughout the day before reducing in intensity overnight, we examined decadal changes in nighttime vapor pressure deficits over the western United States with a focus on the summer fire season. We calculated changes using a recently updated observation-assimilating reanalysis (ERA5) available at hourly resolution over the 1980–2019 period. Analysis identifies the proximate cause (atmospheric temperature vs. moisture content) of the observed changes and the extent to which they have been captured in climate model simulations. Increases in nighttime vapor pressure deficits of >50% in 40 years are evident over foothills of mountains ranges adjacent to arid plateaus. The largest observed increases greatly exceed the forced climate-model response. Correlation analysis reveals a broad link between the variability of western US summer-nighttime vapor pressure deficit and the Pacific Decadal Oscillation.

Plain Language Summary Western US wildland fire managers have reported that fires are burning longer into the night and increasing in intensity earlier in the morning compared to when many started their careers. Increasing nighttime vapor pressure deficit—a measure of the *drying power* of air—is widely suspected to be responsible for these perceived changes in fire behavior. It is also suspected that human-caused increases in nighttime temperatures are responsible. We used a recently released observation-based data set to quantify the extent to which nighttime vapor pressure deficits have changed over the last 40 years and determine the proximate cause for the observed changes (particularly whether temperature effects on their own can explain them). We also explored how well the observed changes are captured in climate model simulations. Results highlight large increases in nighttime vapor pressure deficit over the foothills of mountain ranges next to arid plateaus, where the observation-based increases greatly exceed the climate model projections, and both temperature and humidity play a role in driving the observed changes.

1. Introduction

Vapor pressure deficit (VPD) is defined as the difference between the saturation (VPS) and actual (VP) vapor pressures and can be interpreted as the "drying power" of air (Monteith & Unsworth, 2008). Wildland fuels dry more rapidly as deficits and wind speeds increase (Anderson, 1936; Penman, 1948). When combined with higher wind speeds, dry fuels increase the risk of fires spreading rapidly (McDonald et al., 2018; Srock et al., 2018).

VPD has been used to rationalize the observed interannual variability in burned area over many western US regions. For example, Williams et al. (2014) found that spring-summer VPD correlated with annual burned area over the Southwest at least as well as 14 other fire-related variables. Seager et al. (2015) found strong correlations between interannual variability of summertime VPD and burned area in southwestern US forests ($r = 0.8$) and grasslands ($r = 0.62$). Williams et al. (2019) found that California summertime burned area variability is substantially correlated with warm-season VPD ($r = 0.72$), especially over forests ($r_{forest} = 0.79$; $r_{non-forest} = 0.35$). Because historical fire information is generally limited to start date, location and total area burned (e.g., Eidenshink et al., 2007) most studies relating weather and climate variability to fire behavior have focused on aggregated metrics (e.g., annual means over a region). One exception is the study of Sedano and Randerson (2014), which used satellite-derived (Giglio, 2010) daily fire perimeters over Alaska to reveal

correlations between daily VPD variability at forest-fire locations with other fire metrics including ignition probability, daily spread and extinction.

Our interest in nighttime VPD is motivated by a perception among many western US wildland fire managers that, compared to a few decades ago, fires are picking up in intensity earlier in the morning or are burning later into the evening before exhibiting reduced intensity and rates of spread overnight. Increases in nighttime VPD over the last four decades are suspected to play a role in this perceived change in fire behavior. Particularly, increased nighttime VPD, other factors equal, will increase the rates at which fuels dry at night or hinder fuel moisture recovery in the case that sufficient sources of moisture (e.g., dew or soil moisture) are available (Potter, 2012; Seager et al., 2015).

Daily mean estimates from observation-assimilating numerical weather models, a.k.a. *reanalysis*, indicate that VPD has increased over recent decades across most of the United States (Ficklin & Novick, 2017; Seager et al., 2015). Some of the largest increases occurred during summer over the southwestern United States, where they have been linked to unusually active wildfire seasons (Williams et al., 2014) and escalations in regional wildfire activity over this same period (Abatzoglou & Williams, 2016; Williams et al., 2019).

VPS varies strongly with air temperature. For example, it doubles when air temperature increases from 283 K (~50°F) to 294 K (~70°F). Karl et al. (1993) found that nighttime temperatures since the 1950s were increasing 3× faster than daytime temperatures over half of the land in the northern hemisphere (cf. Easterling et al., 1997). Subsequent studies have found that global nighttime and daytime temperatures have risen at comparable rates since the Karl et al. (1993) study period (Thorne et al., 2016; Vose et al., 2005), but also that the Southwest has experienced large nighttime temperature increases compared to continental-scale averages over recent decades (Davy et al., 2017; Qu et al., 2014). This motivates our initial question about the extent to which enhanced nighttime temperature increases over the western United States may be affecting nighttime VPD. We are not aware of previous studies that have documented nighttime VPD change.

We are ultimately interested in better understanding the degree to which the VPDs during recent summer fire seasons might be substantially different from earlier periods, especially at night. We used hourly data from a recently developed reanalysis (ERA5, Hersbach et al., 2020) to examine the extent to which nighttime VPD has changed over western US summers (July–September). VPD changes were calculated between *recent* and *earlier* periods, defined as 2010–2019 and 1980–1999. These periods were chosen to represent conditions during the most recent decade and during the period in which many current firefighters began their careers and formed concepts of historically normal wildfire conditions. Our analysis identifies the proximate cause (temperature effects on VPS or changes in actual VP) for the observed changes and how the nighttime results compare to those based on daily averaged data. We also compared the observation-based results with the simulations for this same period from climate models integrated under the influence of increasing atmospheric carbon dioxide (CO_2) concentration. This was to better understand the extent to which the effects of rising atmospheric CO_2 levels, as they are represented by the climate-model mean, can explain the observed changes in VPD.

2. Data and Methods

VPS and VP were calculated using near surface (2 m) temperature (T) and dew point temperature (T_d) from the European Centre for Medium Range Forecasting ERA5 reanalysis and formulae recommended by Alduchov and Eskridge (1996). Specifically,

$$e_s = 6.109 \times e^{\left(\frac{17.625 \times T}{T + 243.04}\right)} \tag{1}$$

$$e_a = 6.109 \times e^{\left(\frac{17.625 \times T_d}{T_d + 243.04}\right)} \tag{2}$$

$$\text{VPD} = e_s - e_a \tag{3}$$

wherein e_s represents VPS, e_a represents actual VP and temperatures input in °C yield vapor pressures in hPa. ERA5 T and T_d were downloaded on a 0.25° latitude × 0.25° longitude grid and hourly resolution. Hourly vapor pressures were calculated from the hourly temperature and dew point temperature data. Summertime-daily (24-h) and summer-nighttime averages of VPS, VP, and VPD were calculated based on the corresponding hourly data. Herein, nighttime is defined as 05:00–12:00 Coordinated Universal Time (UTC). ERA5's hourly resolution is a factor 3–24 improvement over other popular reanalysis-derived, fire-weather data sets (cf. Seager et al., 2015; Sedano & Randerson, 2014; Williams et al., 2019). This facilitates our examination of nighttime conditions with ERA5.

Period differences are reported in both absolute units and normalized change relative to the earlier period. The daily average normalized period difference is calculated as

$$\text{normalized period difference} = \frac{\text{VPD}_2 - \text{VPD}_1}{\text{VPD}_1} \tag{4}$$

where VPD_2 is summer-daily VPD averaged over our recent period and VPD_1 is the average over our earlier period.

The contribution of nighttime VPS and VP change to the normalized period difference in nighttime VPD is calculated by the following decomposition:

$$\frac{n\text{VPD}_2 - n\text{VPD}_1}{n\text{VPD}_1} = \frac{ne_{s2} - ne_{s1}}{n\text{VPD}_1} + \frac{-1 \times \left(ne_{a2} - ne_{a1}\right)}{n\text{VPD}_1} \tag{5}$$

where the abbreviations and symbols retain their previous definitions and the prefix, n, indicates nightly values in the summertime.

Monthly climate model VPD data were acquired from the University of Idaho Northwest Knowledge Web site. The data are from 20 models contributed to the 5th Coupled Model Intercomparison Project (CMIP5; Taylor et al., 2012) and have been bias corrected and downscaled to 4 km resolution using methods described by Abatzoglou (2013) and Abatzoglou and Brown (2012). The CMIP5-based results shown here are based on relaxing the model atmospheric CO_2 concentration to observations over the historical period (1950–2005) and to Representative Concentration Pathway 4.5 (RCP4.5) concentrations over the projected period (Thomson et al., 2011). RCP8.5 results are also available from this archive. However, we used RCP4.5 because RCP4.5 concentrations have tracked observations more closely (10× less projected-period bias) than RCP8.5 (Figure S1). Individual CMIP5-model results contain components forced by rising greenhouse gas concentrations and internal sources of variability. Averaging over all bias-corrected model results is believed to offer the best-available estimate of the forced signal (Frankcombe et al., 2018), which is what we wish to compare to the observations.

3. Results

July through September constitutes the core fire season over most of the western United States. Daily averaged VPD averaged over these months of each year from 1980 to 2019 is shown in Figure 1a. Peak deficits are seen across the lower Colorado River basin, where summertime-averaged temperatures exceed 34°C. VP would need to exceed 55 hPa here to reach saturation. Rather, they range from 10 hPa near the Nevada-New Mexico border to 16 hPa along the southern California-New Mexico border. This leaves a deficit of about 40 hPa along the southern core of the Colorado River basin (Figure 1a). Deficits in the 20–30 hPa range are seen over other relatively warm regions including California's central (Sacramento and San Joaquin) valley, where average summertime temperatures exceed 25°C, and over much of the Great Basin, Columbia River Basin, and Snake River Basin.

Changes between recent (2010–2019) and earlier (1980–1999) periods based on daily averaged VPD reveal a period difference maximum in the 6–10 hPa range over the San Juaquin Valley and adjacent foothills of the southern Sierra Nevada (Figure 1b). Secondary maxima of 4–6 hPa are seen at lower elevations of the Columbia River and Snake River Basins. Much of the Southwest has experienced changes of >2 hPa, including
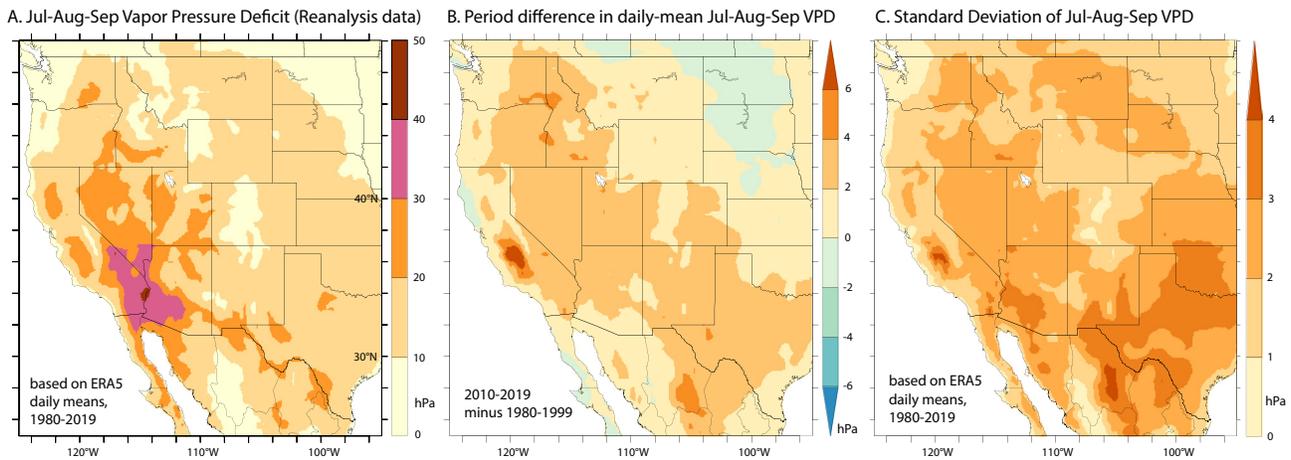
Figure 1. (a) July–August–September vapor pressure deficit (VPD) based on daily averaged observation-based reanalysis results. (b) Difference in July–August–September daily mean VPD between the most recent decade (2010–2019) and first two decades (1980–1999) of our study period. (c) Standard deviation of July–August–September daily mean VPD during 1980–2019.

nearly all of Nevada and Utah, and much of Arizona, New Mexico, Colorado, and Texas. Period differences >2 hPa extend to northern California, Oregon, Washington, Idaho, and Montana.

Before considering nighttime, we compare daily averaged observational (reanalysis) results with the estimated change forced by rising greenhouse gas concentrations over our study period; that is, the bias-corrected CMIP5 multi-model mean. Using daily averaged reanalysis data facilitates this comparison with the CMIP5 results, which are available at daily but not sub-daily resolution.

The daily averaged, observation-based period difference shown in Figure 1b is repeated in Figure 2a after normalizing by the earlier period-mean VPD. Recent-period, daily averaged fire-season VPD has risen more than 30% above the earlier period mean in many sub-regions. These include the San Joaquin Valley and western flanks of the southern Sierra Nevada and Rocky Mountain foothills covering parts of Oregon,
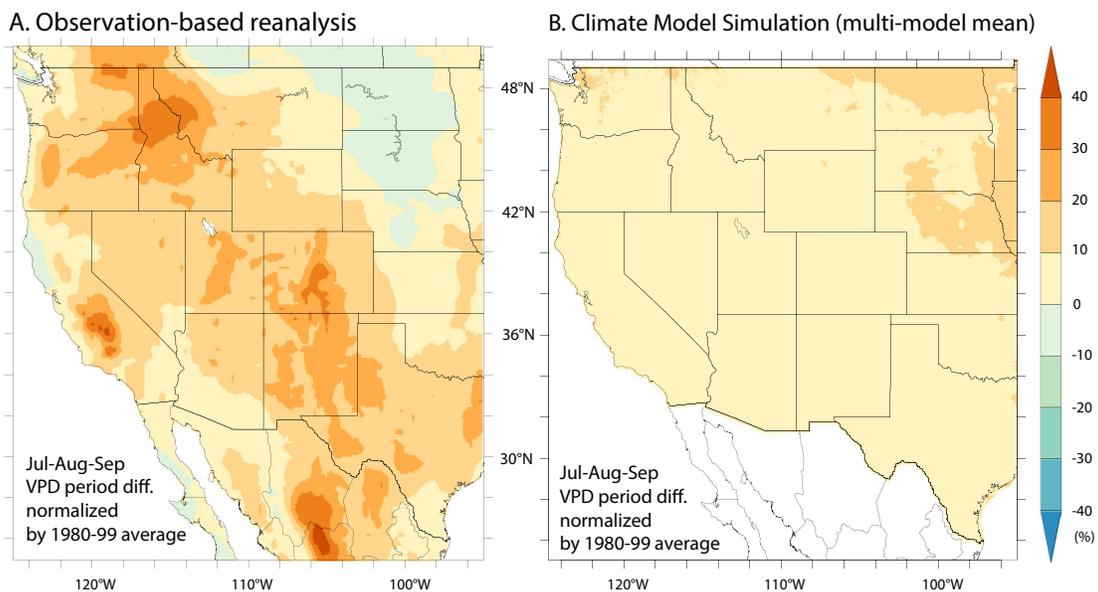

Figure 2. Difference in daily summertime vapor pressure deficit (VPD) between recent (2010–2019) and earlier (1980–1999) periods, normalized by the earlier-period average. Panel (a) shows observation-based reanalysis results. Panel (b) shows our estimate (5th Coupled Model Intercomparison Project multi-model mean) of the climate-model forced response.
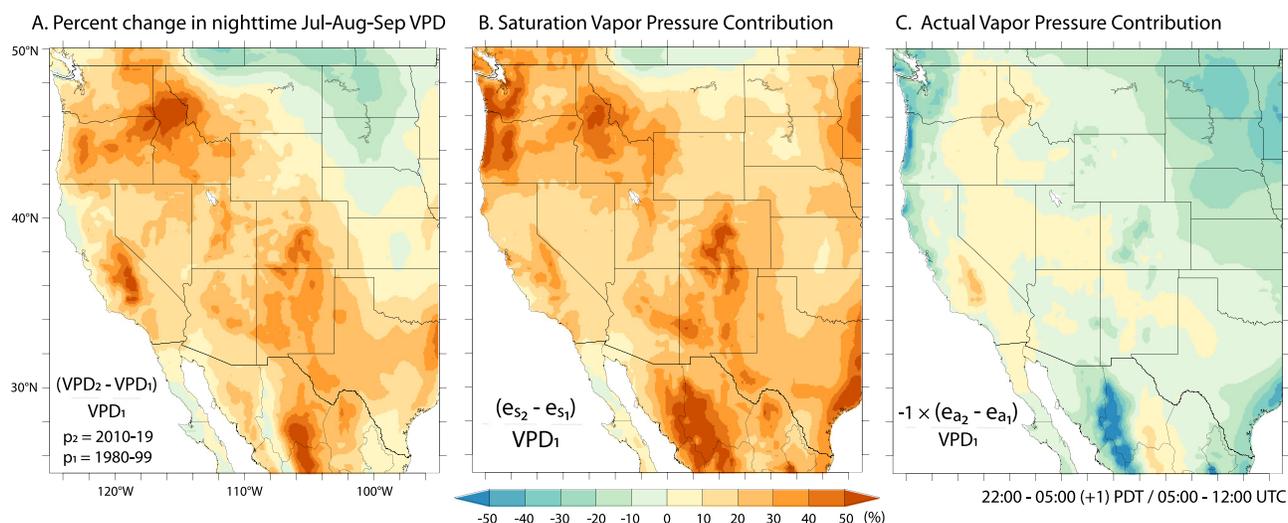
Figure 3. (a) Percent change in 2010–2019 nighttime July–August–September vapor pressure deficit (VPD) relative to the 1980–1999 period, based on ERA5 data. (b and c) show the period differences in July–August–September nighttime VPS (e_s) and $-1 \times$ VP (e_a) normalized by the same factor as in Figure 3a, namely, nighttime July–August–September VPD averaged over the earlier period. Hence, results in (a) = (b) + (c).

Washington, Idaho, Montana, and Colorado. Daily averaged VPD increases exceeded 20% of the earlier period mean over ~20% of the land area shown in Figure 2a.

The mean change simulated over this period by the climate models is much lower in amplitude and different in character from the observation-based estimate. The mean-simulated change in VPD (Figure 2b) nowhere exceeds 20% of the earlier period mean and exceeds 10% over only about 10% of the study region, mainly over the northern Mississippi River Basin. Over the area of the western United States that has, based on the reanalysis data, experienced an increase of 30% or greater, the mean-simulated change averages 7.5%. Averaged over this same area the observation-based increase in summer-daily VPD is 4.6 times greater than the climate model mean (cf. Figures 2a and 2b). Over western US forests and woodlands (Figure S2), the observation-based change averages 18% and reaches maxima of 39% over the forested flanks of the Idaho Rocky Mountains and southern Sierra Nevada. Over these same areas, the mean-simulated change averages 7% and reaches maxima of only 9%–10%.

The amplitude of the observation-based VPD increases stand out even when compared to the range of results among the individual models in the CMIP5 archive: For example, the observed increases exceed the CMIP5-mean by >1 model-archive standard deviation over 53% of the western United States and exceed the maximum increase produced by any of the 20-individual climate models over 29% of the western United States (Figure S3).

The nighttime July–August–September VPD change based on reanalysis data is shown in Figure 3a, with values given as percent change between the recent and earlier period. Increases exceeding 50% of the earlier-period mean are seen over the western flanks of the southern Sierra Nevada as well as a larger region spanning the flanks of the Bitterroot sub-range of the Rocky Mountains in Idaho and Blue Mountains of eastern Oregon and Washington. Increases exceeding 50% of the earlier-period mean are also evident over the Mexican States of Chihuahua and Durango.

These regional maxima cover mountainous terrain adjacent to lower elevation plateaus, namely the Columbia River Basin in the Northwest and San Joaquin Valley of California, where long-term average VPDs are much larger than over the adjacent higher elevations (cf. Figure 1a). According to the reanalysis data, decadal-mean nighttime VPDs that were typical at mid-elevations in the earlier period have climbed to higher elevations in the recent period. For example, the 6 hPa nighttime VPD isobar running along the western flanks of the Idaho Rocky Mountains moved from a mean elevation of 1,060 m (3,500 ft) in the earlier period to an elevation of 1,650 m (5,400 ft) in the recent decade. The characteristic VPD at 1,650 m was 4 hPa in the earlier period.

Similarly, in the southern Sierra Nevada, nighttime VPD averaged over the earlier period was characterized by a 4 hPa isobar running along the western mountain flanks at an average elevation of 2,300 m (7,500 ft). The earlier period 6 hPa isobar traversed this region to the west of the 4 hPa isobar at a lower mean elevation of 1,660 m (5,500 ft). Over the recent period, the 6 hPa isobar has risen to approximately the mean elevation of the earlier period 4 hPa VPD isobar.

Figures 3b and 3c show the normalized contributions from VPS and VP change, which added together equate to the VPD change shown in Figure 3a. Specifically, Figures 3b and 3c illustrate the second and third terms of Equation 5.

Nighttime VPS (Figure 3b) has increased over 98% of the study region. Because VPS is a function of temperature, it follows that nighttime temperatures have increased over a similarly large portion of the study region. Using the reanalysis data, we looked into the question of whether increases in nighttime temperature have outpaced increases in daily average temperature. Comparison of nighttime-averaged versus daily averaged temperature changes between the two periods revealed that the answer depends on location (see Figure S4).

Over 67% of the study region, nighttime temperatures have risen faster than daytime temperatures. This has occurred over nearly all of Washington, Oregon, Idaho, California, Nevada, Arizona, and New Mexico, and parts of Utah, Texas, Montana, and Wyoming. The area with enhanced nighttime temperature increase includes the Rocky Mountain maximum in VPD change. Over this local maximum, defined by increases in Figure 3a exceeding 50%, nighttime averaged temperatures have increased by 2.0°C between the recent and earlier periods and daily averages have increased by 1.8°C.

A given *change* in air temperature, however, will cause a greater change in saturation vapor pressure at a higher temperature (e.g., during the day) than it will at a comparatively lower temperature (e.g., during the night). Thus, even though nighttime temperature rise has outpaced daytime temperature rise over the Rocky Mountain maximum, the local increase between recent and earlier periods in daily average VPS (2.2 hPa) is slightly larger than nighttime (2.1 hPa).

Over the Sierra Nevada maximum, nighttime and daily average temperatures have risen by 1.8°C and 1.5°C, respectively, between the earlier and recent periods. Here, the earlier-to-recent period increase in daily average VPS (2.2 hPa) is slightly smaller than the nighttime increase (2.3 hPa).

Two other aspects of the nighttime changes over these regions drew our attention. The first is that decadal scale VP change has contributed to the period difference in VPD over these regions. This is not the case over most of the study region. VP increases (negative/blue hues in Figure 3c) cover 75% of the land in our study area. These increases in VP effectively buffer the changes in VPD that would have otherwise been caused by increases in VPS driven by rising temperatures. Such buffering is simulated by the CMIP5 models (Figure S5) over all land in our study region and is especially strong in the observations over western Washington and Oregon. Over the Rocky Mountain maximum, however, observations show that decreasing VP contributed approximately one-fifth of the total regional average increase in VPD of 57%. Over the Sierra Nevada maximum, decreases in VP account for 40% of the observed increase of 53%.

The second aspect of interest over the Rocky Mountain and Sierra Nevada maxima is that VPDs were relatively low in magnitude and year-to-year variability in the earlier period compared to the increases evident in the recent period (the period differences in nighttime VPD, normalized by the standard deviation of summer-nighttime VPD within the earlier period, are shown in Figure S6). This is especially evident over the Sierra Nevada maximum, where the summer with the *lowest* nighttime average VPD in the most recent decade (8.7 hPa in 2011) is still more than 0.5 hPa above the *highest* seen in the first two decades of the study period (8.2 hPa in 1981). Over this region, the mean change between periods is up to 5× larger than the standard deviation of the 20 summer-nighttime averages seen in the earlier period (cf. Figure 4 and Figure S6).

Correlation analysis reveals that the observed variability in summer-nighttime VPD is linked ($r = -0.61$) to variability of the Pacific Decadal Oscillation (PDO; see Figure 4 inset). The PDO is defined by the leading principal component of North Pacific sea surface temperature (Mantua et al., 1997) and has previously been associated with both cold and warm-season US precipitation variability (e.g., Mantua & Hare, 2002;
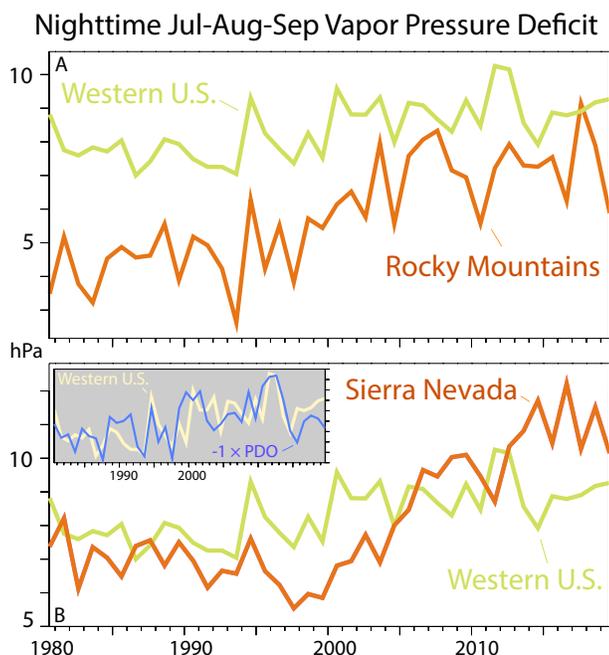
Nighttime Jul-Aug-Sep Vapor Pressure Deficit

Figure 4. Summer-nighttime averaged vapor pressure deficit, 1980–2019. The *western US* curve shows the study region average. The *Sierra Nevada* and *Rocky Mountain* curves illustrate averages over these region's maxima, defined by increases between the recent (2010–2019) and earlier (1980–1999) periods >50% of the earlier period mean. The panel (b) inset shows the *western US* curve with summertime (July–August–September) values of the Pacific Decadal Oscillation (PDO) index (normalized to unit standard deviation).

Zhao et al., 2017). We find, based on statistical methods similar to those used by Rudnick and Davis (2003), that the observed correlation between July–August–September PDO and regionally averaged nighttime VPD variability is statistically significant at the 95% confidence interval (period 1980–2019; see Figure S6 and corresponding discussion in the Supplemental Material). Further examination shows that the summer-time PDO correlation with summer-nighttime VPD, VPS, and *T* is mainly of one sign (negative) across the western United States, with strongest magnitudes ($|r| > 0.6$) over the interior Northwest (see Figures S7a, S7b and S7d). The PDO correlation with VP, however, changes sign across the region and has smaller-magnitude maxima than the VPD and VPS correlation maps. Evidently, the regionally averaged nighttime VPD-PDO correlation is mainly contributed by temperature effects on VPS.

4. Summary and Discussion

Vapor pressure deficit is known to affect fire behavior by influencing the rates at which fuels dry (Potter, 2012; Seager et al., 2015). The results presented here indicate that substantial increases in vapor pressure deficit have taken place over many western US regions, including the foothills of mountain ranges adjacent to arid plateaus where daily average vapor pressure deficits have increased by >30% and nighttime by >50% over the last 40 years.

Firefighters experience longer workdays and get less rest between shifts when fires do not reduce intensity at night. Western US firefighters report that this problematic scenario has been occurring with increasing frequency. The results presented here support the hypothesis strongly held already by many wildland managers that increasing nighttime vapor pressure deficits are responsible for increasingly long fire days. More work is needed, however, to quantify meteorological anomalies and evaluate impacts on fire behavior at the specific dates and locations of the fires in question. Doing this reliably will require expanding upon the generally available fire records (e.g., Eidenshink et al., 2007) to include more detailed information about day-to-day (and day-to-night) behavior during the lifetimes of wildfires.

The CMIP5 multi-model mean underestimates the amplitude and fails to reproduce the pattern of the increases in vapor pressure deficit observed since the 1980s. This demonstrates, to the extent the CMIP5 results capture the forced effects of rising atmospheric CO_2, that other sources of decadal-timescale variability have dominated changes in vapor pressure deficit seen since the period (1980s and 1990s) when many current firefighters formed their concepts of normal fire behavior. Pacific Decadal Oscillation variability is, evidently, substantially linked to broad, regionally coherent, changes in vapor pressure deficit across the western United States. This source of decadal variability does not, however, fully explain the largest observed increases adjacent to the southern Sierra Nevada and Rocky Mountains. Further study is needed to better understand the mechanisms for this decadal variability and their predictability.

For many areas of the western United States, increases in actual vapor pressure have buffered the impact that would have resulted from temperature-driven increases in saturation vapor pressure on their own. The changes to date in nighttime vapor pressure deficits have been greatest, however, along the foothills of mountain ranges adjacent to arid plateaus where decreases in actual vapor pressures have contributed to the evident increases in vapor pressure deficit. Understanding whether this upslope creep of aridity will continue, and at what rate, will be critical to understanding the extent to which higher elevation forests, that to date have been relatively humid at night, will be impacted by the effects of drier nights in the future.

These results motivate further study to better understand the reasons for this upslope creep in aridity. More study is also needed to quantitatively link changes in vapor pressure deficit with fuel moisture variability and impacts on fire behavior. Reducing the uncertainty associated with these endeavors will likely require

increased investment in sustained, high-quality observations of fire behavior and fire-related weather and fuel moisture variables.

Data Availability Statement

The CMIP5-based data are available at http://thredds.northwestknowledge.net:8080/thredds/reacch_climate_CMIP5_aggregated_macav2_monthly_catalog.html (Accessed August 4, 2020). ERA5 data are available at https://www.ecmwf.int/en/forecasts/datasets/reanalysis-datasets/era5 (Accessed July 2, 2020). Monthly PDO values are available at https://stateoftheocean.osmc.noaa.gov/atm (Accessed May 1, 2021).

References

Abatzoglou, J. T. (2013). Development of gridded surface meteorological data for ecological applications and modelling. *International Journal of Climatology*, *33*, 121–131. https://doi.org/10.1002/joc.3413

Abatzoglou, J. T., & Brown, T. J. (2012). A comparison of statistical downscaling methods suited for wildfire applications. *International Journal of Climatology*, *32*, 772–780. https://doi.org/10.1002/joc.2312

Abatzoglou, J. T., & Williams, N. P. (2016). Impact of anthropogenic climate change on wildfire across western US forests. *Proceedings of the National Academy of Sciences*, *113*(42), 11770–11775. https://doi.org/10.1073/pnas.1607171113

Alduchov, O. A., & Eskridge, R. E. (1996). Improved magnus form approximation of saturation vapor pressure. *Journal of Applied Meteorology*, *34*, 601–609. https://doi.org/10.1175/1520-0450(1996)035<0601:IMFAOS>2.0.CO;2

Anderson, D. B. (1936). Relative humidity or vapor pressure deficit. *Ecology*, *17*, 277–282. https://doi.org/10.2307/1931468

Davy, R., Esau, I., Chernokulsky, A., Outten, S., & Zilitinkevitch, S. (2017). Diurnal asymmetry to the observed global warming. *International Journal of Climatology*, *37*, 79–93. https://doi.org/10.1002/joc.4688

Easterling, D. R., Horton, B., Jones, P. D., Peterson, T. C., Karl, T. R., Parker, D. E., et al. (1997). Maximum and minimum temperature trends for the globe. *Science*, *277*, 364–367. https://doi.org/10.1126/science.277.5324.364

Eidenshink, J. C., Schwind, B., Brewer, K., Zhu, Z.-L., Quayle, B., & Howard, S. M. (2007). A project for monitoring trends in burn severity. *Fire Ecology*, *3*, 3–21. https://doi.org/10.4996/fireecology.0301003

Ficklin, D. L., & Novick, K. A. (2017). Historic and projected changes in vapor pressure deficit suggest a continental scale drying of the United States atmosphere. *Journal of Geophysical Research: Atmospheres*, *122*, 2061–2079. https://doi.org/10.1002/2016JD025855

Frankcombe, L. M., England, M. H., Kajtar, J. B., Mann, M. E., & Steinman, B. A. (2018). On the choice of ensemble mean for estimating the forced signal in the presence of internal variability. *Journal of Climate*, *31*(14), 5681–5693. https://doi.org/10.1175/JCLI-D-17-0662.1

Giglio, L. (2010). *MODIS collection 5 active fire product user's guide version 2.4* (pp. 1–60). Science Systems and Applications Inc., University of Maryland, Department of Geography.

Hersbach, H., Bell, B., Berrisford, P., Hirahara, S., Horányi, A., Muñoz-Sabater, J., et al. (2020). The ERA5 global reanalysis. *Quarterly Journal of the Royal Meteorological Society*, *146*, 1999–2049. https://doi.org/10.10002/qj.380310.1002/qj.3803

Karl, T. R., Jones, P. D., Knight, R. W., Kukla, G., Plummer, N., Razuvayev, V., et al. (1993). A new perspective on recent global warming: Asymmetric trends of daily maximum and minimum temperature. *Bulletin of the American Meteorological Society*, *74*(6), 1007–1023. https://doi.org/10.1175/1520-0477(1993)074<1007:anporg>2.0.co;2

Mantua, N. J., & Hare, S. R. (2002). The Pacific decadal oscillation. *Journal of Oceanography*, *58*, 35–44. https://doi.org/10.1023/A:1015820616384

Mantua, N. J., Hare, S. R., Zhang, Y., Wallace, J. M., & Francis, R. C. (1997). A Pacific interdecadal climate oscillation with impacts on salmon production. *Bulletin of the American Meteorological Society*, *78*(6), 1069–1079. https://doi.org/10.1175/1520-0477(1997)078<1069:apicow>2.0.co;2

McDonald, J. M., Srock, A. F., & Charney, J. J. (2018). Development and application of a Hot-Dry-Windy Index (HDW) climatology. *Atmosphere*, *9*, 285. https://doi.org/10.3390/atmos9070285

Monteith, J. L., & Unsworth, M. H. (2008). *Principles of environmental physics* (p. 418). Elsevier.

Penman, H. L. (1948). Natural evaporation from open water, bare soil and grass. *Proceedings of the Royal Society A*, *193*, 120–145. https://doi.org/10.1098/rspa.1948.0037

Potter, B. E. (2012). Atmospheric interactions with wild land fire behavior—I. Basic surface interactions, vertical profiles and synoptic structures. *International Journal of Wildland Fire*, *21*, 779–801. https://doi.org/10.1071/WF11128

Qu, M., Wan, J., & Hao, X. (2014). Analysis of diurnal air temperature range change in the continental United States. *Weather and Climate Extremes*, *4*, 86–95. https://doi.org/10.1016/j.wace.2014.05.002

Rudnick, D. L., & Davis, R. E. (2003). Red noise and regime shifts. *Deep-Sea Research*, *50*, 691–699. https://doi.org/10.1016/s0967-0637(03)00053-0

Seager, R., Hooks, A., Williams, A. P., Cook, B., Nakamura, J., & Henderson, N. (2015). Climatology, variability, and trends in the U.S. Vapor pressure deficit, an important fire-related meteorological quantity. *Journal of Applied Meteorology and Climatology*, *54*(6), 1121–1141. https://doi.org/10.1175/jamc-d-14-0321.1

Sedano, F., & Randerson, J. T. (2014). Multi-scale influence of vapor pressure deficit on fire ignition and spread in boreal forest ecosystems. *Biogeosciences*, *11*, 3739–3755. https://doi.org/10.5194/bg-11-3739-2014

Srock, A. F., Charney, J. J., Potter, B. E., & Goodrick, S. L. (2018). The Hot-Dry-Windy Index: A new fire weather index. *Atmosphere*, *9*, 279. https://doi.org/10.3390/atmos9070279

Taylor, K. E., Stouffer, R. J., & Meehl, G. A. (2012). An overview of CMIP5 and the experiment design. *Bulletin of the American Meteorological Society*, *93*, 485–498. https://doi.org/10.1175/BAMS-D-11-00094.1

Thomson, A. M., Calvin, K. V., Smith, S. J., Kyle, G. P., Volke, A., Patel, P., et al. (2011). RCP4.5: A pathway for stabilization of radiative forcing by 2100. *Climatic Change*, *109*, 77–94. https://doi.org/10.1007/s10584-011-0151-4

Thorne, P. W., Donat, M. G., Dunn, R. J. H., Williams, C. N., Alexander, L. V., Caesar, J., et al. (2016). Reassessing changes in diurnal temperature range: Intercomparison and evaluation of existing global data set estimates. *Journal of Geophysical Research: Atmospheres*, *121*, 5138–5158. https://doi.org/10.1002/2015JD024584

Vose, R. S., Easterling, D. R., & Gleason, B. (2005). Maximum and minimum temperature trends for the globe: An update through 2004. *Geophysical Research Letters*, *32*, L23822. https://doi.org/10.1029/2005GL024379

Williams, A. P., Abatzoglou, J. T., Gershunov, A., Guzman-Morales, J., Bishop, D. A., Balch, J. K., & Lettenmaier, D. P. (2019). Observed impacts of anthropogenic climate change on wildfire in California. *Earth's Future*, *7*, 892–910. https://doi.org/10.1029/2019EF001210

Williams, A. P., Seager, R., Berkelhammer, M., Macalady, A. K., Crimmins, M. A., Swetnam, T. W., et al. (2014). Causes and implications of extreme atmospheric moisture demand during the record-breaking 2011 wildfire season in the southwestern United States. *Journal of Applied Meteorology and Climatology*, *53*(12), 2671–2684. https://doi.org/10.1175/jamc-d-14-0053.1

Zhao, S., Deng, Y., & Black, R. X. (2017). Observed and simulated spring and summer dryness in the United States: The impact of the Pacific Sea surface temperature and beyond. *Journal of Geophysical Research: Atmosphere*, *122*, 12713–12731. https://doi.org/10.1002/2017JD027279

References From the Supporting Information

Masarie, K. A., & Tans, P. P. (1995). Extension and integration of atmospheric carbon dioxide data into a globally consistent measurement record. *Journal of Geophysical Research*, *100*, 11593–11610. https://doi.org/10.1029/95jd00859

Meinshausen, M., Smith, S. J., Calvin, K., Daniel, J. S., Kainuma, M. L. T., Lamarque, J.-F., et al. (2011). The RCP greenhouse gas concentrations and their extensions from 1765 to 2300. *Climatic Change*, *109*, 213–241. https://doi.org/10.1007/s10584-011-0156-z

Riahi, K., Rao, S., Krey, V., Cho, C., Chirkov, V., Fischer, G., et al. (2011). RCP 8.5—A scenario of comparatively high greenhouse gas emissions. *Climatic Change*, *109*, 33–57. https://doi.org/10.1007/s10584-011-0149-y